GENERALISATION OF EFFECTIVE HEAVE PRESSURE CONSIDERING THE EFFECT OF SMALL-STRAIN STIFFNESS

Tornborg, J.[1], Karlsson, M.[2], Kullingsjö, A.[3], Abed, A.[4] and Karstunen, M.[5]

KEYWORDS

Excavation, clay, earth pressure, heave, numerical modelling

ABSTRACT

Excavation in low-permeable soils is typically followed by delayed heave during consolidation, which is often restrained by a structural element, affecting the earth pressure. In this paper, system insights on the mechanisms that control heave pressure are complemented by investigating the effect of small-strain stiffness. This is enabled by an extension of the Creep-SClay1S model that considers small-strain stiffness. It is shown that the effect of small-strain stiffness and its degradation with shear strains can be normalized by considering a two-dimensional time factor, a geometrical influence factor and the initial stiffness in the mid-point of the clay layer beneath the excavation. The results provide guidance on how consideration of small-strain stiffness affect effective heave pressure, in addition to factors such as excavation geometry, thickness of clay layer and normalised construction time. The results can be used in preliminary design and to complement project-specific analyses. Overall, the research contributes to a deeper understanding of excavation induced earth pressures and, thus, reduces the uncertainty and enables to optimize the volumes of construction materials.

[1] Skanska Sverige AB, Göteborg, Sweden.
[2] Chalmers University of Technology, Göteborg, Sweden.
[3] Skanska Sverige AB, Göteborg, Sweden.
[4] Chalmers University of Technology, Göteborg, Sweden.
[5] Chalmers University of Technology, Göteborg, Sweden.

1. INTRODUCTION

Excavation invokes excess pore pressure changes which in low-permeable soils manifest as delayed heave during consolidation. If such a heave process is restrained by a structural element, an earth pressure will form. This pressure was referred to as the effective heave pressure, EHP, by [1]. During the design of Göta Tunnel in Gothenburg in 2001, earth pressure due to restrained heave against the bottom slab was considered and project-specific analyses were carried out by an expert investigation [2]. Such project-specific analyses are typically limited to major infrastructure projects as they are time-consuming.

Recently, an objective of a research project at Chalmers University of Technology [3] was to generalise the formation of EHP on underground structures in deep excavations in soft clay. The methodology utilised dimensional analysis. A parametric study, conducted with the Finite Element Method using the Creep-SClay1S model [4,5] was synthesised and presented in charts using appropriate non-dimensional parameter groups. The approach enables scaling of the results, making them applicable for a wide range of settings and projects.

In this paper, the system insights on the mechanisms that control effective heave pressure are complemented by investigating the effect of small-strain stiffness. This is enabled by a recent extension [6,7] of the Creep-SClay1S model. The results provide guidance on how consideration of small-strain stiffness affects EHP in addition to factors such as excavation geometry, thickness of clay layer, normalized construction time (time, coefficient of consolidation, drainage length).

2. CONSIDERED SOIL-STRUCTURE SYSTEM

Idealized geometry

The effect of considering small-strain stiffness in the assessment of effective heave pressure is studied for an idealized *Tunnel* geometry, see Figure 1. The slab and the retaining wall are modelled as rigid and the ground water table is located at the excavation base. This simplified scenario was complemented in [3] with a scenario involving the ground water table located 1m below ground surface level. The results were similar; hence the simplified scenario is re-analysed here to study the effect of considering small-strain stiffness. Similar to [3] the lower boundary and slab-clay interface are considered permeable, whereas the horizontal boundaries are impermeable.

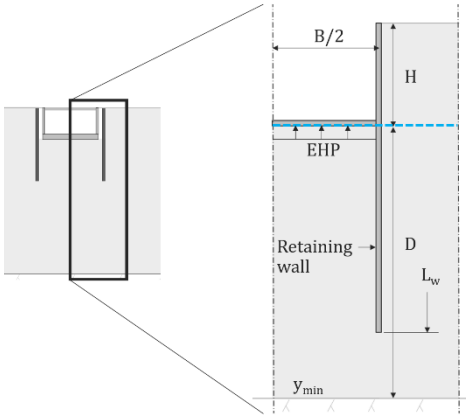

Figure 1 Idealized plane strain Tunnel geometry studied in this paper.

In [3] dimensional analysis was used to form dimensionless groups of the variables considered in the studied system. Furthermore, a two-dimensional time factor T_{2D} was introduced:

$$T_{2D} = [(t_{exv.\text{-}slab} * c_v)/((y_{min}\text{-}H)/2)^2 + (2B/y_{min})(t_{exv.\text{-}slab} * c_h)/(B/2)^2] / 2 \text{ [-]} \quad \text{Eq. 1}$$

T_{2D} is also used in this paper to compile the results of the finite element simulations in which the following variables are varied: the time between the excavation and casting the slab $t_{exv.\text{-}slab}$ (5, 30, 90, 365 days), depth of excavation H (5 and 10 m, with length of the wall L_w=15 m and 25 m, respectively), width of the excavation B (10, 25, 50 m) and the distance to the bearing stratum y_{min} (25, 50, 75, 100 m).

Constitutive model

In this paper a formulation of the Creep-SClay1S model that accounts for non-linear degradation of stiffness with shear strain [7] is used, here referred to as Creep-SClay1S-s. [7] also accounted for strain accumulation under cyclic loading which is not included in the model formulation used in this paper. In Creep-SClay1S-s the secant shear modulus G decays from a reference small-strain shear modulus G_0 with shear strain ε_q as suggested by [6] according to:

$$G = G_0 \left[1 - \frac{\langle \varepsilon_q - \varepsilon_s \rangle}{A + B\langle \varepsilon_q - \varepsilon_s \rangle}\right] \quad \text{Eq. 2}$$

where ε_s is a threshold value set to 10^{-5}, A is a model parameter controlling the degradation and B defined according to:

$$B = \frac{1}{1 - \frac{G_{ur}}{G_0}} \quad \text{Eq. 3}$$

where G_{ur} is the stiffness determined by e.g. unloading-reloading in incremental loading oedometer tests. The small-strain feature of the model thus requires input of two additional parameters, *A* and *ssMP* with *ssMP*=κ^*/κ_0^* (i.e. a small-strain multiplier and the inverse of G_{ur}/G_0).

Parameter *A* is estimated to 0.001 based on data found in the literature, see Figure 2, using a plasticity index (PI) typical for Gothenburg clay i.e. in the range of 30-40% (see e.g. [8]) and with *ssMP*=5. Eq. 2 with *A*=0.001 and *ssMP* in the range 5-10 also agree well with field and laboratory data presented by [11] on Bäckebol clay (just north of Gothenburg) where the PI was reported to be in the range 30-40%.

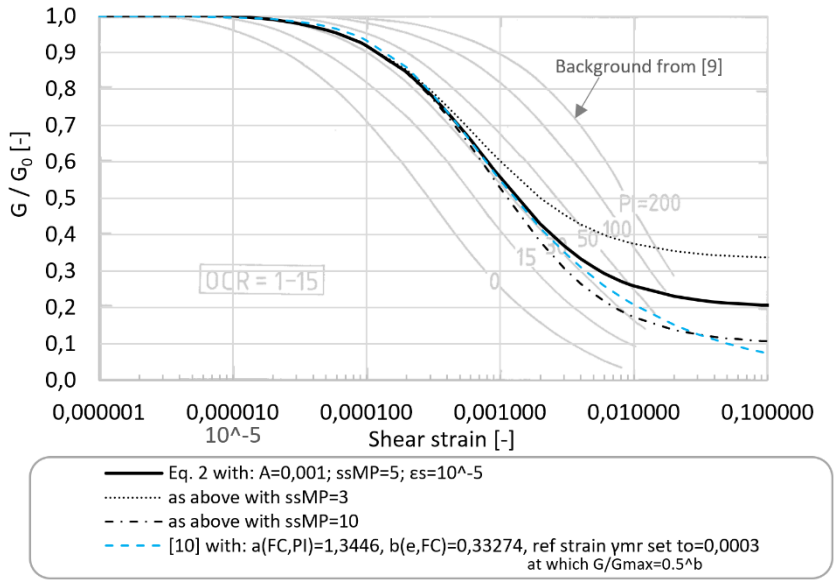

Figure 2. Illustration and estimation of parameters A and ssMP based on plasticity index.

Taking κ^*=0.015 and *ssMP*=5 result in an attainable range of stiffness as illustrated in Figure 3 for the initial mean effective stress profile considered in this example and a Poisson's ratio of 0.20.

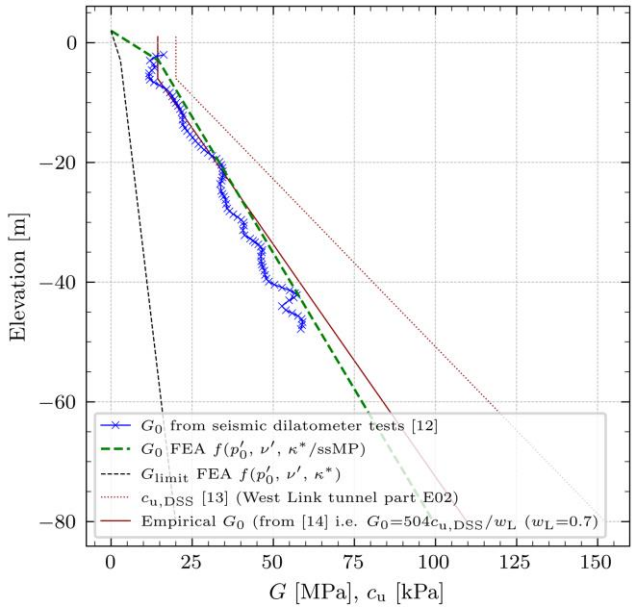

Figure 3. Comparison of measured and empirical G_0 in Gothenburg to initial and limiting stiffness (at large shear strains, from Eq. 2) in the finite element simulations.

The parameters of the Creep-SClay1S-s model are summarised in Table 1 with additional input parameters vertical overconsolidation ratio *OCR*=1.3, earth pressure coefficient at-rest K_0=0.6 and permeability (hydraulic conductivity) k_v=k_h=10^{-9} m/s.

Table 1. Creep-SClay1S-s model parameter values.

Parameter	Description	Value
γ/γ' [kN/m3]	Bulk/submerged unit weight	16/6
λ_i^* [-]	Modified intrinsic compression index	0.07
κ^* [-]	Modified swelling index	0.015
ν' [-]	Poisson's ratio	0.20
M_c [-]	Slope of CSL in triaxial compression	1.45
M_e [-]	Slope of CSL in triaxial extension	1.10
ω [-]	Rate of rotational hardening	200
ω_d [-]	Relative rate of rotational hardening due to dev. strain	1
a [-]	Rate of destructuration	8
b [-]	Relative rate of destructuration due to dev. strain	0.5
α_0 [-]	Initial anisotropy	0.57
χ_0 [-]	Initial amount of bonding	15
μ_i^* [-]	Modified intrinsic creep index	1/550
τ [days]	Reference time	1
K_0^{nc}	Earth pressure coefficient at primary loading	0.42
ssMP [-]	Small-strain stiffness multiplier	5
A [-]	Shape factor for stiffness degradation	0.001

3. RESULTS

An example illustrating the degradation of stiffness in the model domain is presented in Figure 4 for two of the finite element simulations with B=50 m, y_{min}=75 m. In Figure 4a $t_{exv\text{-}slab}$=5 days i.e. the excavation remained open for 5 days before the restraining slab was cast and in Figure 4b this time was 365 days. Hence, the degradation of stiffness has more time to develop (due to increasing shear strains). A detail in Figure 4 is the somewhat greater reduction in stiffness behind the retaining wall in Figure 4a compared to Figure 4b. This is explained by considering that in Eq. 2, the degradation of stiffness is solely dependent on the total deviatoric strain. By checking the value of ε_q in the simulations shown in Figures 4a and 4b it is confirmed that ε_q behind the wall was in fact reducing somewhat with time (from 5 to 365 days).

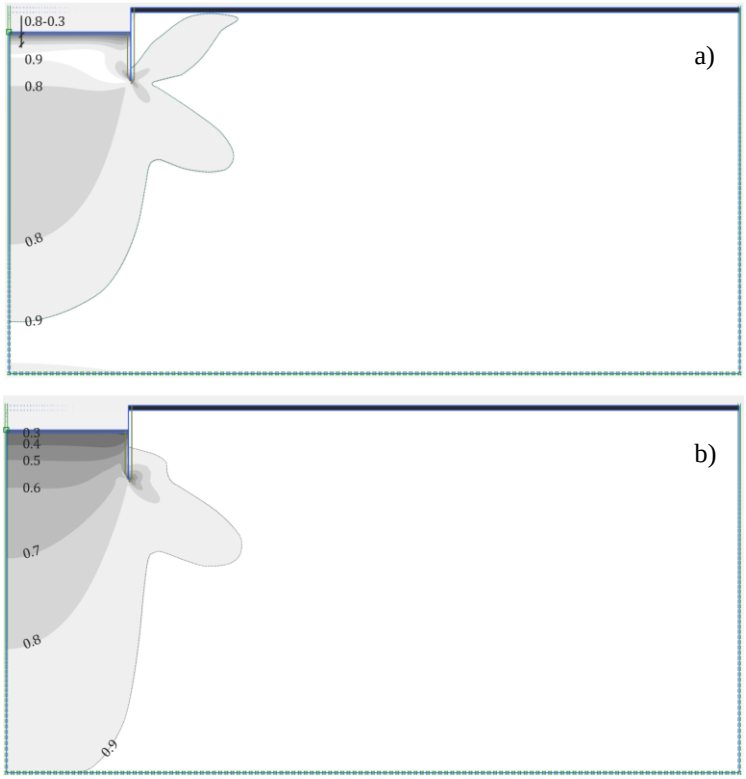

Figure 4. Example of stiffness degradation illustrated by G/G_0 at the time before application of slab for two of the simulations included in Figure 5: a) $t_{exv\text{-}slab}$=5 days, and b) $t_{exv\text{-}slab}$=365 days.

The results of the finite element simulations are compiled in Figure 5 presenting the effective heave pressure at the central location of the slabs, $\sigma'_{n,centr}$. A key to reading the colours and markers of Figure 5 is provided in Table 2. The

intention is not, however, to be able to separate the result of single simulations, rather it is to study the range of the normalised results.

Simulations with the small-strain Creep-SClay1S-s model are overlaid (red symbols) on the results from [3] (using the Creep-SClay1S and SClay1S models). The plotted results from the simulations with the creep models are maximum values occurring typically within 10 years after the activation of the slab in these simulations. In the case of narrow excavations, however, these maximum values reduce in the long-term due to background creep settlements causing "down drag". For further details of the effect of background settlements see [3]).

The results are normalized with the *initial* stiffness in the middle of the clay layer (between the excavation base and the lower model boundary). For the Creep-SClay1S-s model κ_0^* is used to calculate the initial stiffness. For simulations with equal settings except for the small-strain stiffness formulation, the normalisation shifts the Creep-SClay1S-s results to the right due to the higher initial stiffness.

In Figure 5b, the simulations with T_{2D}<0.02 are replotted to derive an influence factor μ_i (similar to estimation of initial settlement "influence factors" [15]) which describes that one part of the heave will be instant, and another part delayed, depending on the extent of the excavation in relation to the depth of the clay layer. (see further details in [3]).

In Figure 5c the results are normalized by μ_i. Figure 5c indicates that the results of Creep-SClay1S and Creep-SClay1S-s are comparable, however, when T_{2D}>0.1 the Creep-SClay1S-s results are somewhat higher. This is explained by the fact that when the normalized time increases, e.g. if the excavation remains open for a longer time before the slab is activated, the stiffness is given more time to degrade. Hence normalisation using the initial small-strain stiffness shifts the results somewhat excessively to the right, most notably when T_{2D}>0.1. The agreement of the results normalized by μ_i and T_{2D} is still considered satisfactory, which provides further credibility to the presented charts as well as partial validation of the recent implementation of non-linear stiffness in the Creep-SClay1S model.

Table 2. Key to colours and markers for in Figure 5.

Parameter	Variation	Unit
y_{min}	25, 50, 75, 100	m
B	10(□), 25(◁), 50(◇)	m
H	5, 10[a)]	m
$t_{exc.-slab}$	5, 30, 90, 365	days

Red symbols = Creep-SClay1S-s, other Creep-SClay1S and SClay1S.
[a)] half-filled symbols

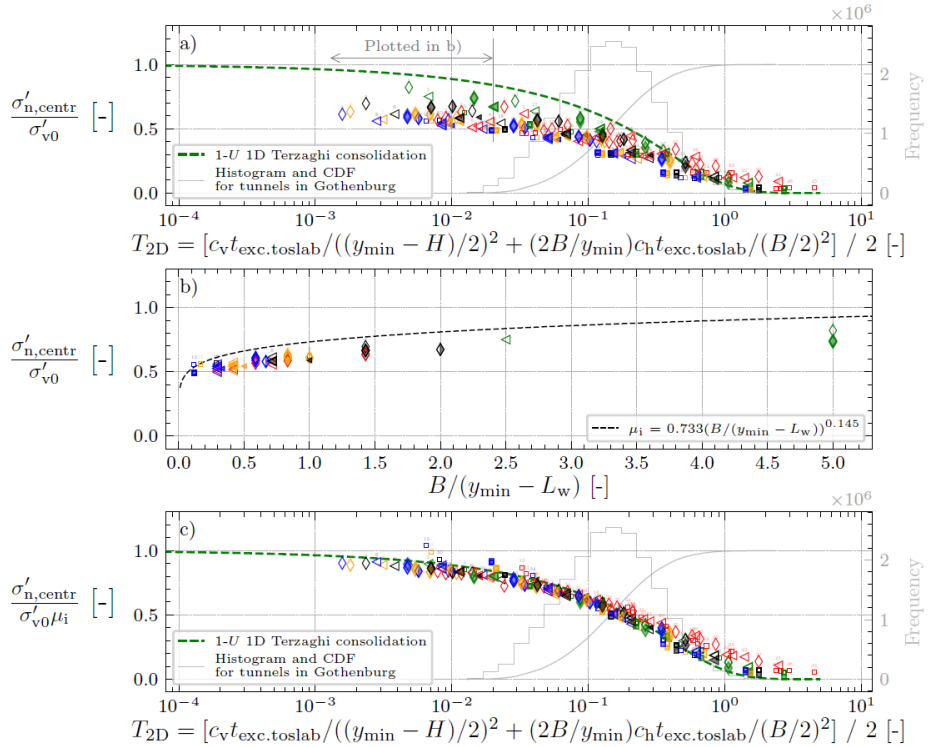

Figure 5. Data from [3] complemented with results of small strain stiffness and histogram and cumulative distribution function (CDF) for fictive tunnels in Gothenburg: a) EHP-ratio at central part of slab plotted against T_{2D}, b) geometrical influence factor μ_i, and c) EHP-ratio normalised by μ_i and plotted against T_{2D}.

A histogram and cumulative distribution function (CDF) illustrating typical values T_{2D} for a tunnel construction in Gothenburg is included in Figure 5. The histogram was constructed drawing 10 random values from each of the ranges presented in Table 2 (except for 20 values for *k*). The CDF tells us that the EHP-ratio is in the range 0.3--0.5 for the median T_{2D} value. The recommendation is, however, that the engineers use charts such as Figure 5 to estimate the magnitude of the EHP for the specific project at hand.

Table 3. Ranges used to construct the histogram and cumulative distribution function for typical tunnels in Gothenburg.

Variable	Range	Unit
H	5--15	m
B	20--40	m
y_{min}	30--100	m
E at top of clay layer	10--20	MPa
E_{inc}	0.5--2.0	MPa/m
$k_v = k_h$	10^{-10}--10^{-9}	m/s
$t_{exc.-slab}$	90--365	days

4. CONCLUSIONS

When excavating in low-permeable soils, a delayed heave process is triggered that, if restrained, will introduce an earth pressure on the restraining structural element. This earth pressure is referred to as the effective heave pressure, EHP, and has previously been studied in detailed project specific analyses for Göta Tunnel in Gothenburg. In this paper, the effect of considering small-strain stiffness on EHP in deep excavations in soft clay was examined to complement recently published results from a finite element parametric study synthesized into non-dimensional design charts [3]. The effect of small-strain stiffness was studied by the recently developed Creep-SClay1S-s model.

The results show that by considering a two-dimensional time factor T_{2D} and a geometrical influence factor, the results of the parametric study can be normalized by the initial soil stiffness in the clay layer even when considering small-strain stiffness and its degradation due to accumulated shear strains.

The results provide guidance on how consideration of small-strain stiffness affect effective heave pressure in addition to factors such as excavation geometry, thickness of clay layer, normalized construction time (time, coefficient of consolidation, drainage length). The results contribute to a deeper understanding of excavation induced earth pressures and, thus, reduce uncertainty and enable to optimise the volumes of construction materials.

The model parameters describing the small-strain stiffness and its degradation were estimated based on empirical data found in the literature. Hence, it is recommended to study the degradation of small-strain stiffness for soft Swedish clays further, to attain representative values for the small-strain stiffness parameters.

ACKNOWLEDGEMENTS

The authors gratefully acknowledge the financial support provided Skanska, SBUF (the Development Fund of the Swedish Construction Industry, Grant 13995), BIG (Better Interaction in Geotechnics, Grant A2021-06, from the Swedish Transport Administration) and Formas (Grant 2019-00456).

REFERENCES

[1] Simpson, B.: Effective heave pressures beneath restrained basement slabs. Proceedings of the Institution of Civil Engineers - Geotechnical Engineering, 171(1), 28–36, 2018. https://doi.org/10.1680/jgeen.16.00066

[2] Alén, C., & Sällfors, G.: Utredning rörande svälltryck mot pålad bottenplatta [Investigation regarding heave pressure acting on piled foundation slab]. SGI & Chalmers University of Technology, 2001.

[3] Tornborg, J.: On the temporal evolution of earth pressure in deep excavations in soft clay. PhD thesis, Chalmers University of Technology, 2024.

[4] Sivasithamparam, N., Karstunen, M., & Bonnier, P.: Modelling creep behaviour of anisotropic soft soils. Computers and Geotechnics, 69, 46–57, 2015. https://doi.org/10.1016/j.compgeo.2015.04.015

[5] Gras, J.-P., Sivasithamparam, N., Karstunen, M., & Dijkstra, J.: Permissible range of model parameters for natural fine-grained materials. Acta Geotechnica, 13(2), 387–398, 2018. https://doi.org/10.1007/s11440-017-0553-1

[6] Sivasithamparam, N., D'Ignazio, M., Tsegaye, A. B., Castro, J., & Madshus, C.: Small strain stiffness within logarithmic contractancy model for structured anisotropic clay. IOP Conference Series: Earth and Environmental Science, 710(1), 012042, 2021. https://doi.org/10.1088/1755-1315/710/1/012042

[7] Tahershamsi, H., Ahmadi Naghadeh, R., Zuada Coelho, B., and Dijkstra, J.: Low amplitude strain accumulation model for natural soft clays below railways. Transportation Geotechnics, 42, 101011, 2023. https://doi.org/10.1016/j.trgeo.2023.101011

[8] Tornborg, J., Karlsson, M., & Dijkstra, J.: Temporal effective stress response of soil elements below the base of an excavation in sensitive clay. Canadian Geotechnical Journal, 2024. https://doi.org/10.1139/cgj-2023-0355

[9] Vucetic, M. and Dobry, R.: Effect of Soil Plasticity on Cyclic Response. Journal of Geotechnical Engineering, 117(1), 89–107, 1991. https://doi.org/10.1061/(ASCE)0733-9410(1991)117:1(89)

[10] Wang, Y. and Stokoe, K. H.: Development of Constitutive Models for Linear and Nonlinear Shear Modulus and Material Damping Ratio of Uncemented Soils. Journal of Geotechnical and Geoenvironmental Engineering, 148(3), 2022. https://doi.org/10.1061/(ASCE)GT.1943-5606.0002736

[11] Andréasson, B. A.: Dynamic Deformation Characteristics of a Soft Clay. Int. Conf. on Recent Advances in Geotechn. Earthquake Eng. and Soil Dynamics, St. Louis, 1981. https://scholarsmine.mst.edu/icrageesd/01icrageesd/session01b/3

[12] Wood, T.: Phase 3 – Site Characterization and Sensitivity Analysis Region City. Technical report, Chalmers University of Technology, 2014.

[13] Trafikverket, NCC, Cowi.: Redogörelse för konstruktionsarbetets förutsättningar och metoder (RKFM) - E02 – Station centralen. Trafikverket, 2019 (granskningshandling).

[14] Larsson, R., Mulabdic, M.: Shear moduli in Scandinavian clays. SGI report 40, 1991.

[15] Janbu, N., Bjerrum, L., Kjærnsli, B.: Veiledning ved løsning av fundamenteringsoppgaver. NGI publikasjon 16, NGI, 1956.